Tropical African wildfire aerosols Trigger Teleconnections in the mid-high latitude of Northern Hemisphere in Boreal Winter

Huiping Yan[1], Zhiwei Zhu[1], Kai Zhang[2], Jingjia Luo[1], Yun Qian[2], and Yiquan Jiang[3]

[1]Nanjing University of Information Science and Technology
[2]Pacific Northwest National Laboratory
[3]Nanjing University

November 24, 2022

Abstract

This study investigates the impacts of wildfire aerosols (primary organic carbon, black carbon and sulfate) on the Northern hemispheric boreal winter climate. We found that wildfire aerosols emitted from equatorial Africa result in two mid-high latitude Rossby wave trains. One is from subtropical Atlantic propagating northward across Europe to Siberia, and the other one propagates eastward from Mid-East across Asia to Northwest Pacific. The maximum positive height anomaly locates in Europe, concurrent with a greater-than-2K surface warming. These Rossby wave trains are excited by the atmospheric heating in equatorial Africa and propagate into extratropics with the help of the westerly jet. Through the heat budget analysis, the source of the Rossby wave is primarily due to the solar absorption of black carbon in Africa. The present study emphasize that aerosols especial the absorbing aerosols would have profound thermo-dynamic effects on remote regions and need more attentions.

Tropical African wildfire aerosols Trigger Teleconnections in the mid-high latitude of Northern Hemisphere in Boreal Winter

Huiping Yan[1], Zhiwei Zhu[1], Bin Wang[2,1], Kai Zhang[3], Jingjia Luo[1], Yun Qian[3], Yiquan Jiang[4]

[1]School of Atmospheric Sciences, Nanjing University of Information Science and Technology, Nanjing, China
[2]Department of Meteorology, University of Hawaii at Manoa, Honolulu, Hawaii, USA
[3]Pacific Northwest National Laboratory, Richland, Washington, USA
[4]School of Atmospheric Sciences, Nanjing University, Nanjing, China

Key Points:

- Significant changes in circulations and temperature in mid-high latitude are induced by African wildfire aerosols in January.
- These effects are imposed through Rossby wave trains excited by the aerosols-induced atmospheric heating anomaly.
- The anomalous atmospheric heating is primarily due to the absorption of solar radiation by black carbon.

Corresponding author: Huiping Yan, `yanhp2009@126.com`

Abstract

[This study investigates the impacts of wildfire aerosols (primary organic carbon, black carbon and sulfate) on the Northern hemispheric boreal winter climate. We found that wildfire aerosols emitted from equatorial Africa result in two mid-high latitude Rossby wave trains. One is from subtropical Atlantic propagating northward across Europe to Siberia, and the other one propagates eastward from Mid-East across Asia to Northwest Pacific. The maximum positive height anomaly locates in Europe, concurrent with a greater-than-2K surface warming. These Rossby wave trains are excited by the atmospheric heating in equatorial Africa and propagate into extratropics with the help of the westerly jet. Through the heat budget analysis, the source of the Rossby wave is primarily due to the solar absorption of black carbon in Africa. The present study emphasize that aerosols especial the absorbing aerosols would have profound thermo-dynamic effects on remote regions and need more attentions.]

Plain Language Summary

[Besides the radiative effects, aerosols could have significant thermo-dynamics impacts. With global atmospheric model, we found that African wildfire aerosols induce significant regional circulations and temperature changes in mid-high latitude. The connections between tropics and extratropics were imposed by Rossby waves triggered by the atmospheric heating in Africa. And the pathways of the propagation of two Rossby wave trains were identified, which were correlated with the subtropical jet streams. And for the atmospheric heating, black carbon contributed around 80% to the changes of total solar heating rate. This study emphasized the aerosols especially with absorbing aerosols could result in profound thermo-dynamic effects which need more cautions.]

1 Introduction

Aerosol through scattering and absorbing solar radiation could alter energy balance, and also can be activated as cloud droplet nuclei/or ice nuclei changing the cloud radiative and microphysical properties and affecting the cloud radiative effects. The aerosol radiative effects and aerosol-cloud interaction effects have been widely studied and evaluated, still being a hot topic in the atmospheric community. Besides the radiative effects of aerosols, the radiative forcing of aerosols could further induce regional warming or cooling (e.g., Chen et al., 2016; Ramanathan & Carmichael, 2008; Z. Li et al., 2016), and the persistence of the regional anomalies could further induce large-scale climate response via dynamical or thermal-dynamical effects.

There are lots of studies on the regulation of aerosol effects on regional climate. For example, the deposition of dust and black carbon (BC) on Tibetan plateau made the Tibetan Plateau as an elevated heat pump, which would advance the onset of South Asian monsoon, and affect the position of Mei-yu rain belt in East Asia (Lau et al., 2006). BC emitted over India advance the Indian monsoon onset (Bollasina et al., 2013), increase the pre-monsoon rainfall, and reduce monsoon precipitation (Ganguly et al., 2012)due to the absorbing of solar radiation increasing meridional temperature gradient (Meehl et al., 2008). The impacts of anthropogenic aerosols on East Asian Monsoon has been also studied widely (Y. Q. Jiang et al., 2013; Y. Liu et al., 2009; Z. Li et al., 2016; Song et al., 2014; Qian et al., 2001; Giorgi et al., 2003, 2002; Zhang et al., 2012). A more recent atmosphere-ocean coupled modeling study (Lou et al., 2019) showed that BC heating over mid-latitudes can weaken East Asian monsoon through direct heating and cloud feedbacks. In addition, polluted snow by light-absorbing aerosols over Tibetan Plateau could decrease snow albedo, leading to reduced snow cover that in turn changes the East Asian monsoon circulation (Qian et al., 2011, 2015; Yasunari et al., 2015).

These previous studies were mainly focus on the climate impacts of aerosols on regional regions which are close to the aerosol source regions. A global scale impacts can also be generated, such as the weakening of the Hadley Cell (Allen & Sherwood, 2011; Tosca et al., 2013), and shifts of subtropical Jets (Ming et al., 2011). But only few works reported that a teleconnection may be induced by aerosols. For example, the variations of Sahara dust could induce planetary waves (Rodwell & Jung, 2008). Kim et al. (2006) found that the direct radiative effects of dust and BC could excite a planetary wave spanning from North Africa through Eurasia to the North Pacific in boreal spring. In the above two studies model only simulated the absorbing aerosols, we wonder how the global circulation response when scattering aerosols, and the indirect radiative effects of aerosols are included, whether we could build the same pathways of the aerosol remote effects.

This work is a follow-up study of the global analysis of the wildfire aerosol radiation effects done by (Y. Jiang et al., 2016) in which the direct and indirect of three types of aerosols sulfate, BC, and primary organic matter are included and the indirect of fire aerosols are much larger than the direct effect. This study we focus on the thermo-dynamic effects of wildfire aerosols, the key questions we aim to answer here are that how the remote response of aerosols are formed, whether it is the direct or indirect effects of aerosols trigger the remote effects, and whether it is due to the absorbing aerosols or scattering aerosols. In the present study, sensitivity simulations for the period of 2003-2011 using the aerosol emissions from the Global Fire Emission Datasets version 3.1 (GFED V3.1) are employed to investigate the possible impacts of wildfire aerosols on circulation in January. We focus on the climate response in January for two reasons. First, the wildfire aerosols in January are mainly confined to the northern equatorial Africa. Such a single major source region is more desirable to identify the pathway of the remote climate effects of biomass burning aerosols. Second, the planetary stationary waves are most pronounced in boreal winter. The following parts are organized as below: section 2 give the overview of model and experiments, section 3 present the general radiative effects and circalutation changes, and explore the cause of the teleconnections. Section 4 summary the main results and discussion.

2 Model and Experiment Design

2.1 Model

The Community Atmosphere Model version 5.3 (CAM5.3) (Neale et al., 2010) with the finite volume dynamics core are used. A two-moment cloud microphysics scheme (Morrison et al., 2008) is adopted. The Modal Aerosol Model (MAM4) that consists of four lognormal modes (Aitken, accumulation, coarse, and primary carbon mode) is used to predict aerosol mass and number mixing ratios (X. Liu et al., 2016). The primary carbon mode is included to improve the treatment of microphysical ageing of BC and POM (X. Liu et al., 2016).

2.2 Experiment design

Simulations were carried out from 2003 to 2011 with a horizontal resolution of $0.9° \times 1.25°$ and 30 vertical layers. Sea surface temperatures and sea ice are prescribed. Daily fire emissions are prescribed using the Global Fire Emissions Database version 3.1 (GFED 3.1) (?, ?) for BC, POM and sulfur dioxide (SO2). Anthropogenic aerosol and precursor gas emissions are from the IPCC AR5 dataset (Lamarque et al., 2010). Two sets of 10 ensembles with/without fire aerosols (named as Fire and noFire) are performed. One additional simulation (noBC) was conducted with fire BC emissions turned off to distinguish the effects of absorbing aerosols from the total effects. Other forcings (e.g., SST, greenhouse gases) of all these experiments are kept the same. These simulations are documented in Y. Jiang et al. (2016) and detailed analysis of the aerosol radiative forcing has been provided.

3 Results

3.1 Fire aerosol-induced radiative fluxes

Fig. 1 shows the impact of fire aerosols on the AOD, radiative fluxes, and surface temperature. The maximum changes of AOD (dAOD > 0.25) is located in the equatorial Africa and the downstream region of the entire equatorial Atlantic (Fig. 1a). The fire aerosol effects on the net radiative flux at the top of the atmosphere (dFNET_toa) and at surface (dFNET_sfc) are shown in Fig. 1b,c. The maximum of dFNET_toa (up to $-10W/m^2$) is correlated with the maximum increase of AOD at the downstream Atlantic Ocean. The second largest dFNET_toa (around $-2W/m^2$) is in North Europe, where the increase of AOD is very weak. At surface, dFNET_sfc can be $-20W/m^2$ over the equatorial Atlantic. The large difference between dFNET_sfc and dFNET_toa over the equatorial Atlantic implies that the absorption in the atmosphere is much stronger, when the fire aerosol effect is considered. There are significant changes in surface air temperature (Fig. 1d) in mid- and high- latitude regions of Europe, Northern Russian, and Alaska. However, the changes in AOD and FNET_sfc are not significant in these regions, and the negative change in FNET_toa will result an overall cooling. This suggests that the local changes in radiative fluxes can not explain the surface warming seen in these regions.

We decompose the total aerosol effects at TOA (dFNET_toa) into direct and indirect, and surface albedo effects following the method of Ghan (2013) to understand the direct and indirect effects of aerosols. The total effects (sum of shortwave and longwave radiative effects) are shown in Fig. 2a-d. The indirect effects of aerosols (Fig. 2a), caused by aerosol-cloud interactions and their impact on radiation, are most profound at the downstream Atlantic Ocean with the maximum of up to $-10W/m^2$. The direct effects of aerosols (Fig. 2b), which are mainly due to the direct absorption and scattering of radiation by aerosols, are mostly confined to the regions where AOD are significantly increased. The contrast between all-sky (positive, Fig. 2b) and clear-sky (negative, Fig. 2c) direct effects in tropical Atlantic indicates that clouds enhance the absorption by aerosols above the cloud top (Lu et al., 2018) and it may be responsible to the large uncertainties in evaluating the total effects of aerosols (Boucher et al., 2013). Different from the direct and indirect effects that are mostly confined to the large values regions of dAOD near equator, the surface albedo effects, which are largely contributed by the changes of the snow albedo induced by aerosols, show profound responses in mid-high latitude, such as Europe and North America (dominated by the longwave component, Fig. 2d,f). The significant change in longwave surface albedo effects in Europe (Fig. 2f) is consistent with the surface warming shown in Fig. 1d, i.e., the warming surface emit much more longwave radiation flux and enhance the radiative cooling effects at the TOA.

The above results indicate there are remote responses in radiation and surface air temperature over North Europe and the total TOA radiative forcing are mainly from the surface albedo effects and surface warming. The local radiative effects alone can not explain the significant remote surface warming. In the next subsection, we will explore how these remote responses are generated.

3.2 Fire aerosol-induced teleconnection patterns

As discussed in sec. 1, despite of the radiative effects, aerosols could have significant impacts on circulations due to the non homogeneous spatial distribution radiative forcing. Thus, the response of circulations to wildfire aerosols are analyzed in this section.

The changes of troposphere temperature and geopotential height at 500hPa due to fire aerosols are presented in Fig. 3a. There are significant responses of the circulation and temperature in the mid-high latitude in Northern Hemisphere with large magnitudes at North Atlantic, North Europe, and Gulf of Alaska and the Pacific Northwest.
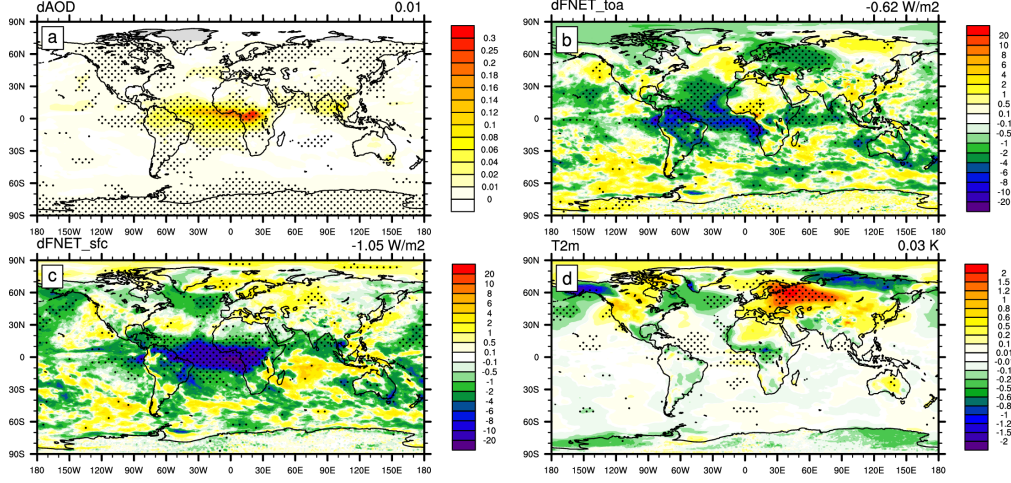
Figure 1. The spatial distribution of aerosol optical depth (dAOD) , the radiative flux at the top of atmosphere (dFNET_toa,W/m2), at surface (dFNET_sfc, W/m2), and 2-meter air temperature (TREFHT, K) due to fire aerosols (95% significant difference is dotted).
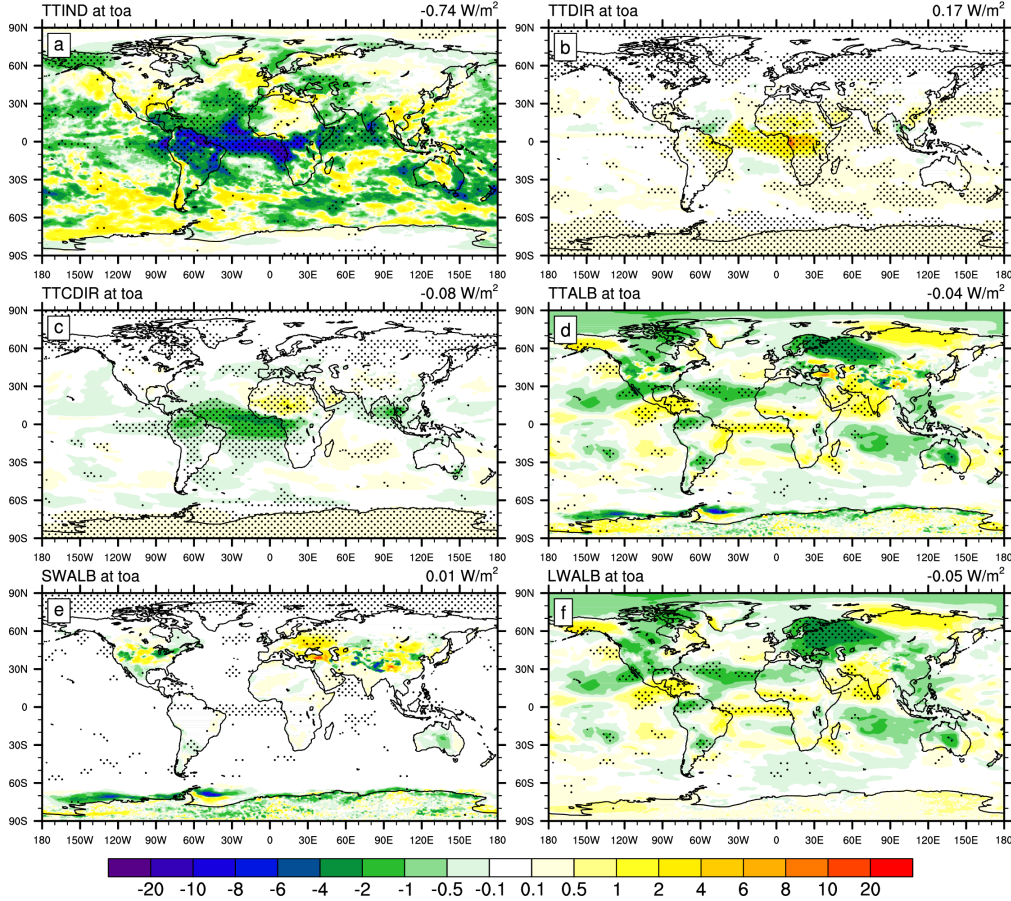

Figure 2. The spatial distribution of total aerosol-cloud interactive effects (TTIND), total direct radiative effects (TTDIR), total direct radiative effects at clear-sky (TTCDIR), total surface albedo effects (TTALB), and the shortwave surface albedo effects (SWALB) and the longwave surface albedo effects (LWALB)(95% significant difference is dotted).

These changes are in wave-train patterns, in which the pattern from North Atlantic across North Europe to Siberia is resembled the Eurasia teleconnection (N. Wang & Zhang, 2015; Y. Liu et al., 2014), and the changes over Alaska, and west coast of North America is a Pacific-North American (PNA)-like pattern (Wallace & Gutzler, 1981; Leathers et al., 1991) that ends at the southeast United States and subtropical North Atlantic. In spatial, the changes of temperature resemble the pattern of geopotential height, where warmer air is concurrent with high pressure anomalies.

At 300hPa, these wave trains can still be found (Fig. 3b). With the zonal wind at 300hPa, we further understand why there are such regional circulation changes. The locations of geopotential heights with small magnitudes from the Mid-East to East Asia are correlated with the subtropical westerly jet over Eurasia. At the outlet of the westerly jet where there are large zonal gradient of the basic state wind, the magnitude of the perturbation is amplified, resulting in significant changes in geopotential height over North Atlantic, North Europe, Alaska, and the west coast of North America.

The vertical structures from Africa, to North Atlantic, Europe, and Siberia are shown in Fig. 3c. In troposphere, it is barotropic for the changes in temperature and geopotential height in troposphere in mid-high latitude. And in the warming regions, there are downward motion while ascending in the cooling regions, indicating the changes of temperature are induced by diabatic heating correlated with the vertical motions. Given the barotropic structure of the stationary wave-train patterns in the anomalous height fields, we inferred that the large-scale circulation anomalies over the mid-high latitudes are linked to stationary Rossby waves that is excited by the fire aerosols in Africa.

The wave activity flux defined in Takaya and Nakamura (2001) are calculated to identify the wave source and the pathways of the wave propagation. There are strong wave activity fluxes from the subtropical Atlantic to North Atlantic and North Europe, and from the gulf of Alaska to the Pacific Northwest and Mexico where large magnitude anomalies locate (see Fig. 3a). And there are weak wave activity fluxes for the wave trains from the Mid-East to East Asia, which are inside of the subtropical jet stream (Fig. 3b). Generally, there are two wave trains, one propagates northeastward to the northeast Atlantic, further eastward to North Europe and Siberia, and the other is a minor branch which propagates eastward to Arabian Peninsula across Mid-East and East Asia, then northward, after reaching its critical latitude (gulf of Alaska), bending equatorward and propagating along the west coast of North America. For the minor branch, it can be found that the westerly jet act as the wave guide for the wave propagation from Mid-East to East Asia. The wave source is the anticyclone in the region of (60-30°W, 20 40°N) located to the northwest of the wildfire aerosol source region, acting as a direct descending Rossby wave response to the low-level African aerosol heating (Gill, 1980).

3.3 Triggers of the teleconnections

From the wave activity flux, we identify the anticyclonic anomaly is the ave source. Based on the theory of Gill-type response(Gill, 1980), the anticyclonic anomaly should be caused by the anomalous heating, which is consistent with the anomalous atmospheric heating in Equatorial Africa (aerosol source region, point A in Fig. 3c). We would like to further verify whether it is this heating that trigger the Rossby wave trains in the mid-high latitude.

A linear anomaly atmosphere general circulation model (AGCM) was employed to study the mechanism of the teleconnection pattern formation. This model was based on the spectrum dry AGCM (Held & Suarez, 1994), which has been used in several studies to reproduce the wave evolution with a specified initial perturbation (Zhu & Li, 2016; R. C. Y. Li et al., 2013). This is baroclinic model with five evenly distributed sigma levels with an interval of 0.2 from 0.9 to 0.1 and a horizontal resolution of T42. The basic mean state (January) is taken from the long-term climatology mean of the National
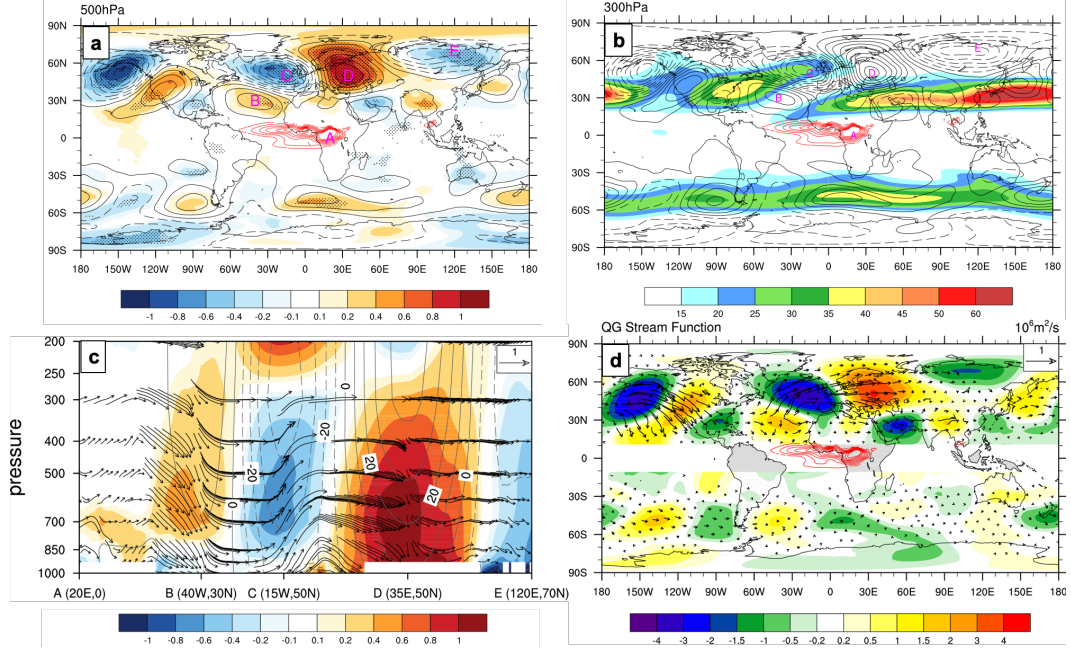
Figure 3. a: The spatial distribution of changes in temperature (color shading) and geopotential height (contour) at 500hPa; b: the spatial distribution of the changes of geopotential height (contour) and zonal mean wind (color shading) from the noFire experiments at 300hPa; c: the vertical cross section of geopotential heigt (contour) and temperature (color shading) and velocity (vector: veritical presssure velocity with units of $-10^{-2}Pa/s$ and horizontal wind speed with units of m/s); d: the spatial distributions of changes in the quasi geostrophic stream function (color shading) and wave activity flux (vector) at 300hPa (95% significant difference is dotted).

Centers for Environmental Prediction–National Center for Atmospheric Research (NCEP–NCAR) reanalysis. A damping rate of $1 day^{-1}$ in the lowest model level ($\sigma = 0.9$) and linearly decaying to $0.1 day^{-1}$ at the middle level ($\sigma = 0.7$) are taken as Rayleigh friction to apply to the momentum equations and to mimic the planetary boundary layer (PBL). Newtonian cooling with an e-folding time scale of 10 days is applied to the temperature equation at all model levels. The heating has a cosine-squared profile in an elliptical region in the horizontal with the maximum rate of $2K/day$.

The time evolution of 300hPa geopotential height response to the specified heating at the Equatorial Africa are shown in Fig. 4. A westward-propagating Gill-type (Gill, 1980) tropical Rossby wave duplet is induced over both sides of the equator to the west of the heating center. Meanwhile, a Gill-type tropical Kelvin wave is also generated at the east of the heating center, propagating eastward. When the westward Rossby wave arrives around $30°N$, it perturbs the westerly jet stream (see Fig. 3b). The westerly jet stream over North Atlantic lead to a northeastward propagation of the stationary Rossby wave, forming a big circle (Hoskins & Ambrizzi, 1993)from the North Atlantic, through Europe to Arctic. The westerly jet stream over Euro-Asia work as the waveguide for the perturbation and transport the perturbation to the East Asia, Pacific, and further to the west of the North America. The wave structure can be clearly seen after day 20 in Fig. 4. As expected, the spatial pattern of the height anomaly resembles that shown in Fig. 3. And this result confirm what we infer above that the atmospheric heating in Africa trigger the Rossby wave trains and large-scale circulation.

For the atmospheric heating over Equatorial Africa, we analysed the adiabatic heating budget over the aerosol source region. Fig. 5a illustrated the profiles of the changes in solar heating rate, longwave heating rate, moist process heating rate, and the temperature tendency from the diffusion. Clearly, for the low level warming over the aerosol source region, solar radiative heating is the most important contributor.

Given the radiative properties of wildfire aerosols we included here, BC is a strong absorbing aerosol which could enhance the absorption of solar radiation. We performed another experiments excluding the wildfire BC (noBC). We can find the solar heating rate is increased when cloud and aerosols, especially BC, are included (Fig. 5b). The magnitude of BC increasing the solar heating rate can be 0.16K/day, which is about 80% to the total aerosol effects on QRS. Thus, we conclude that the absorption of wildfire aerosols by BC are responsible for the anomalous atmospheric heating.

4 Conclusion and discussion

Using the global climate model CAM5, we evaluated the effects of fire aerosols emitted from Equatorial Africa in January. Wildfire aerosols cause significantly negative radiative forcing over the source region and the downwind region over Atlantic, and remote effects in the mid-high latitude with a greater-than-2K warming in North Europe. The remote response is imposed through Rossby wave trains with the circulation changes. Through analyzing the wave active flux and idealized anomalous model simulations, we found that it is the equatorial African aerosol-induced low-level atmospheric heating that result in an anticyclonic anomaly over the subtropical North Atlantic which excites two Rossby wave trains, one along the great circle route via northeast Atlantic and Europe to Siberia and North Pacific and the other along the subtropical jet stream eastward and northeastward with a shorter wave length toward the North Pacific, after reaching its critical latitude (gulf of Alaska), bending equatorward and propagating along the west coast of North America. Among the adiabatic heating budget overt the aerosol source region, the absorption of solar radiation by Black Carbon can contribute 80% to the total changes of solar heating rate that warms the low troposphere and excites the Rossby wave trains.
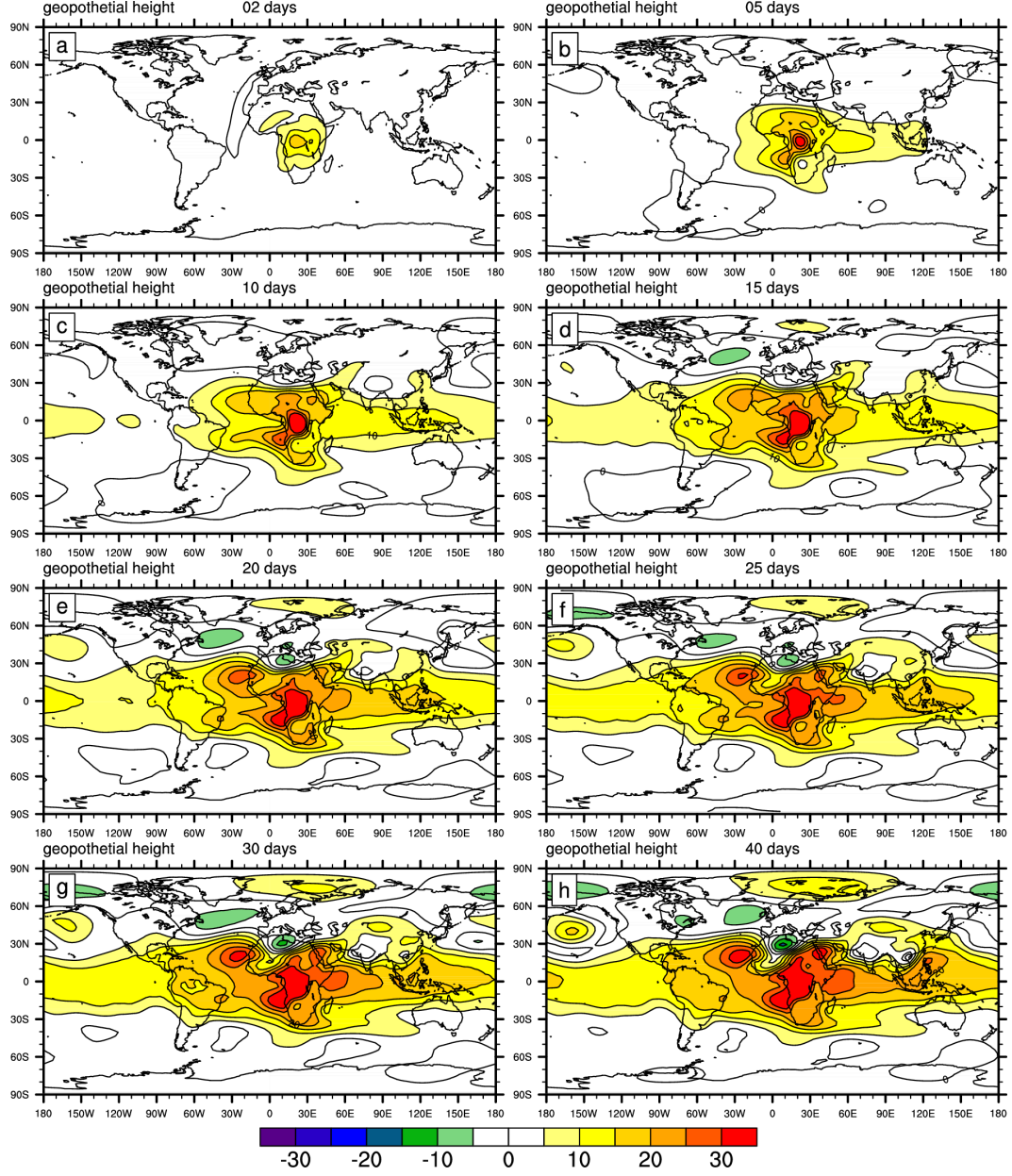
Figure 4. The the temporal evolution of the anomaly in geopotential height at 300hPa using AGCM ideal mode with a heating added in atmosphere in Africa.
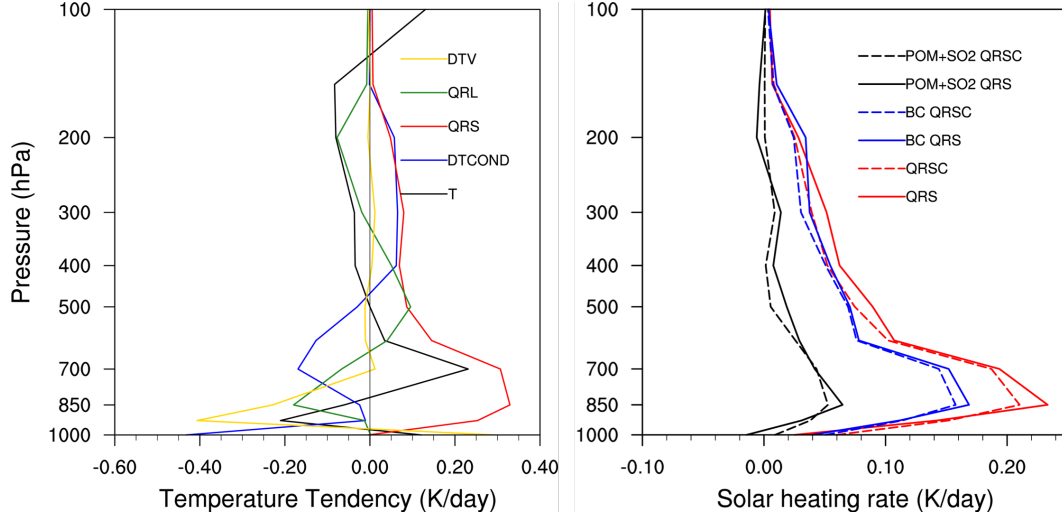
Figure 5. Left: The profiles of changes in adiabatic heating over the source regions. QRS is the solar heating rate, QRL is the longwave heating rate, DTCOND is the temperature tendency caused by moist processes, and DTV is the temperature tendency from the diffusion. T is the temperature with units of K. Right: the profiles of changes in solar heating rate over the source region. The solid line is for all sky, and the dash line is for clear-sky. The BC effects on QRS and QRSC are derived from the difference between Fire and noBC, the POM and SO2 effects are derived from noBC and noFire, and QRS and QRSC are due to all fire aerosols (Fire minus noFire).

Based on the Rossby wave theory, within a tropical easterly flow, Rossby waves hardly escape from the tropics to the extratropics. Thus, how can the equatorial heat source generate extratropical wave trains in this study? As shown in Fig. 3b, the high pressure anomaly responding to the heating in equatorial heating in Africa perturb the westerly jet, and it rapidly grow due to the barotropic instability in the base state on zonal wind (Simmons et al., 1983) and propagate northward into extratropics with the help of the westerly vertical wind shear (B. Wang & Xie, 1996). In addition, the Asian westerly jet act as wave guide to convey the wave energy from Arabia across Mid East, Asia to Pacific and North America.

Besides, the strong negative radiative forcing over the Equatorial Atlantic may further induce low frequency variability. Booth et al. (2012) found the anthropogenic aerosols may contribute to the multi-decadal variability of the Sea Surface Temperature (SSTs) of the North Atlantic Oceans. Amiri-Farahani et al. (2020) using coupled model found the Southern Africa fire aerosols result in a La Nina-like SST response. In this study, as we prescribed SST, the strong cooling effects over the Equatorial Atlantic are suppressed, and thus the Rossby wave trains discussed above is a fast response of the atmosphere. When an ocean model are coupled with the atmospheric model, the cooling effects on the Atlantic SSTs may trigger low frequent variability which would combine the fast response of the atmosphere. But since the inherent barotropic instability of the wind basic state as argued in Simmons et al. (1983), the pathways from the African wildfire aerosols to the remote regions in the mid-high latitude is robust(Fig. A1). We would not go any further for the coupled model results in this study, but it may merit further investigations.

The point we emphasize here is that although the total radiative forcing of wildfire aerosols (c.f. Fig. 2 and Y. Jiang et al. (2016))is cooling, what trigger the planetary

Rossby waves and remote effects is the anomalous atmospheric heating induced by the absorbing aerosols. Thus, the existence of the absorbing aerosols and the thermo-dymamics effects of aerosols may need more cautions and attentions. Further, the 2K surface warming in North Europe in boreal winter could have consequently significant impacts on regional and global climate. The warming surface would enhance snow melting and reduce the snow cover and duration, which would have dramatic effects on the following seasons and further global climate (Bamzai & Shukla, 1999; Barnett et al., 1988).

References

Allen, R. J., & Sherwood, S. C. %. C. D. (2011). The impact of natural versus anthropogenic aerosols on atmospheric circulation in the Community Atmosphere Model. *Climate Dynamics*, *36*(9), 1959–1978. doi: 10.1007/s00382-010-0898-8

Amiri-Farahani, A., Allen, R. J., Li, K., Nabat, P., & Westervelt, D. M. (2020). A La Niña-like climate response to south African biomass burning aerosol in CESM simulations. *Journal of Geophysical Research: Atmospheres*, 1–31. doi: 10.1029/2019JD031832

Bamzai, A. S., & Shukla, J. (1999). Relation between Eurasian snow cover, snow depth, and the Indian summer monsoon: An observational study. *Journal of Climate*, *12*(10), 3117–3132. doi: 10.1175/1520-0442(1999)012⟨3117:RBESCS⟩2.0.CO;2

Barnett, T. P., Dümenil, L., Schlese, U., & Roeckner, E. (1988). The effect of eurasian snow cover on global climate. *Science*, *239*(4839), 504–507. doi: 10.1126/science.239.4839.504

Bollasina, M. A., Ming, Y., & Ramaswamy, V. (2013). Earlier onset of the indian monsoon in the late twentieth century: The role of anthropogenic aerosols. *Geophysical Research Letters*, *40*(14), 3715-3720. doi: 10.1002/grl.50719

Booth, B. B., Dunstone, N. J., Halloran, P. R., Andrews, T., & Bellouin, N. (2012). Aerosols implicated as a prime driver of twentieth-century North Atlantic climate variability. *Nature*, *484*(7393), 228–232. doi: 10.1038/nature10946

Boucher, O., Randall, D., Artaxo, P., Bretherton, C., Feingold, G., Forster, P., . . . others (2013). Clouds and aerosols. In *Climate change 2013: the physical science basis. contribution of working group i to the fifth assessment report of the intergovernmental panel on climate change* (pp. 571–657). Cambridge University Press.

Chen, J. P., Chen, I. J., & Tsai, I. C. (2016). Dynamic feedback of aerosol effects on the East Asian summer monsoon. *Journal of Climate*, *29*(17), 6137–6149. doi: 10.1175/JCLI-D-15-0758.1

Ganguly, D., Rasch, P. J., Wang, H. L., & Yoon, J. H. (2012). Climate response of the South Asian monsoon system to anthropogenic aerosols. *Journal of Geophysical Research-Atmospheres*, *117*. doi: ArtnD1320910.1029/2012jd017508

Ghan, S. J.   (2013).   Technical note: Estimating aerosol effects on cloud radiative forcing. *Atmospheric Chemistry and Physics*, *13*(19), 9971–9974. doi: 10.5194/ acp-13-9971-2013

Gill, A. E. (1980). Some simple solutions for heat-induced tropical circulation. *Quarterly Journal of the Royal Meteorological Society*, *106*(449), 447–462.

Giorgi, F., Bi, X. Q., & Qian, Y.   (2002).   Direct radiative forcing and regional climatic effects of anthropogenic aerosols over East Asia: A regional coupled climate-chemistry/aerosol model study.   *Journal of Geophysical Research-Atmospheres*, *107*(D20). doi: Artn4439Doi10.1029/2001jd001066

Giorgi, F., Bi, X. Q., & Qian, Y.   (2003).   Indirect vs. direct effects of anthropogenic sulfate on the climate of East Asia as simulated with a regional coupled climate-chemistry/aerosol model.   *Climatic Change*, *58*(3), 345–376.   doi: Doi10.1023/A:1023946010350

Held, I. M., & Suarez, M. J.   (1994).   A proposal for the intercomparison of the dynamical cores of atmospheric general circulation models.   *Bulletin - American Meteorological Society*, *75*(10), 1825–1830.   doi: 10.1175/1520-0477(1994) 075⟨1825:APFTIO⟩2.0.CO;2

Hoskins, B. J., & Ambrizzi, T.   (1993).   Rossby wave propagation on a realistic longitudinally varying flow.   *Journal of the Atmospheric Sciences*, *50*(12), 1661–1671.

Jiang, Y., Lu, Z., Liu, X., Qian, Y., Zhang, K., Wang, Y., & Yang, X. Q.   (2016).   Impacts of global open-fire aerosols on direct radiative, cloud and surface-albedo effects simulated with CAM5.   *Atmospheric Chemistry and Physics*, *16*(23), 14805–14824. doi: 10.5194/acp-16-14805-2016

Jiang, Y. Q., Liu, X. H., Yang, X. Q., & Wang, M. H.   (2013).   A numerical study of the effect of different aerosol types on East Asian summer clouds and precipitation.   *Atmospheric Environment*, *70*, 51–63.   doi: 10.1016/j.atmosenv.2012.12.039

Kim, M.-K., Lau, W. K., Chin, M., Kim, K.-M., Sud, Y., & Walker, G. K.   (2006).   Atmospheric teleconnection over eurasia induced by aerosol radiative forcing during boreal spring. *Journal of climate*, *19*(18), 4700–4718.

Lamarque, J. F., Bond, T. C., Eyring, V., Granier, C., Heil, A., Klimont, Z., . . . van Vuuren, D. P.   (2010).   Historical (1850-2000) gridded anthropogenic and biomass burning emissions of reactive gases and aerosols: methodology and application.   *Atmospheric Chemistry and Physics*, *10*(15), 7017–7039.   doi: 10.5194/acp-10-7017-2010

Lau, K. M., Kim, M. K., & Kim, K. M.   (2006).   Asian summer monsoon anomalies induced by aerosol direct forcing: the role of the Tibetan Plateau. *Climate Dynamics*, *26*(7-8), 855–864. doi: 10.1007/s00382-006-0114-z

Leathers, D. J., Yarnal, B., & Palecki, M. A.   (1991).   The pacific/north american teleconnection pattern and united states climate. part i: Regional temperature and precipitation associations. *Journal of Climate*, *4*(5), 517–528.

Li, R. C. Y., Zhou, W., & Li, T.   (2013).   Influences of the Pacific-Japan Teleconnection Pattern on Synoptic-Scale Variability in the Western North Pacific.   *Journal of Climate*, *27*, 140–154. doi: 10.1175/JCLI-D-13-00183.1

Li, Z., Lau, W. K., Ramanathan, V., Wu, G., Ding, Y., Manoj, M. G., . . . Brasseur, G. P.   (2016).   *Aerosol and monsoon climate interactions over Asia* (Vol. 54) (No. 4). doi: 10.1002/2015RG000500

Liu, X., Ma, P. L., Wang, H., Tilmes, S., Singh, B., Easter, R. C., . . . Rasch, P. J.   (2016).   Description and evaluation of a new four-mode version of the Modal Aerosol Module (MAM4) within version 5.3 of the Community Atmosphere Model.   *Geoscientific Model Development*, *9*(2), 505–522.   doi: 10.5194/gmd-9-505-2016

Liu, Y., Sun, J. R., & Yang, B.   (2009).   The effects of black carbon and sulphate aerosols in China regions on East Asia monsoons.   *Tellus Series B-*

398   *Chemical and Physical Meteorology*, *61*(4), 642–656.   doi: DOI10.1111/
399   j.1600-0889.2009.00427.x

400 Liu, Y., Wang, L., Zhou, W., & Chen, W.   (2014).   Three eurasian teleconnection
401   patterns: Spatial structures, temporal variability, and associated winter cli-
402   mate anomalies. *Climate dynamics*, *42*(11-12), 2817–2839.

403 Lou, S., Yang, Y., Wang, H., Smith, S. J., Qian, Y., & Rasch, P. J.   (2019).   Black
404   Carbon Amplifies Haze Over the North China Plain by Weakening the East
405   Asian Winter Monsoon.   *Geophysical Research Letters*, *46*(1), 452–460.   doi:
406   10.1029/2018GL080941

407 Lu, Z., Liu, X. H., Zhang, Z. B., Zhao, C., Meyer, K., Rajapakshe, C., . . . Penner,
408   J. E.   (2018).   Biomass smoke from southern Africa can significantly enhance
409   the brightness of stratocumulus over the southeastern Atlantic Ocean.   *Pro-*
410   *ceedings of the National Academy of Sciences of the United States of America*,
411   *115*(12), 2924–2929. doi: 10.1073/pnas.1713703115

412 Meehl, G. A., Arblaster, J. M., & Collins, W. D.   (2008).   Effects of black carbon
413   aerosols on the Indian monsoon.   *Journal of Climate*, *21*(12), 2869–2882.   doi:
414   Doi10.1175/2007jcli1777.1

415 Ming, Y., Ramaswamy, V., & Chen, G.   (2011).   A Model Investigation of Aerosol-
416   Induced Changes in Boreal Winter Extratropical Circulation.   *Journal of the*
417   *Atmospheric Sciences*, *24*(23), 6077–6091. doi: 10.1175/2011jcli4111.1

418 Morrison, H., Gettelman, A., Morrison, H., & Ghan, S. J.   (2008).   A new two-
419   moment bulk stratiform cloud microphysics scheme in the community atmo-
420   sphere model, version 3 (CAM3). Part I: Description and numerical tests.
421   *Journal of Climate*, *21*(15), 3660–3679. doi: Doi10.1175/2008jcli2105.1

422 Neale, R. B., Chen, C. C., Gettelman, A., Lauritzen, P. H., Park, S., Williamson,
423   D. L., . . . Lamarque, J. F.   (2010).   Description of the NCAR community
424   atmosphere model (CAM 5.0). *NCAR Tech. Note NCAR/TN-486+ STR*.

425 Qian, Y., Flanner, M. G., Leung, L. R., & Wang, W.   (2011).   Sensitivity studies on
426   the impacts of Tibetan Plateau snowpack pollution on the Asian hydrologi-
427   cal cycle and monsoon climate.   *Atmospheric Chemistry and Physics*, *11*(5),
428   1929–1948. doi: 10.5194/acp-11-1929-2011

429 Qian, Y., Giorgi, F., Huang, Y., Chameides, W., & Luo, C.   (2001).   Regional sim-
430   ulation of anthropogenic sulfur over East Asia and its sensitivity to model
431   parameters.   *Tellus Series B-Chemical and Physical Meteorology*, *53*(2), 171–
432   191. doi: DOI10.1034/j.1600-0889.2001.d01-14.x

433 Qian, Y., Yasunari, T. J., Doherty, S. J., Flanner, M. G., Lau, W. K. M., Ming, J.,
434   . . . Zhang, R. (2015). Light-absorbing particles in snow and ice: Measurement
435   and modeling of climatic and hydrological impact.   *Advances in Atmospheric*
436   *Sciences*, *32*(1), 64–91. doi: 10.1007/s00376-014-0010-0

437 Ramanathan, V., & Carmichael, G. (2008). Global and regional climate changes due
438   to black carbon. *Nature Geoscience*, *1*(4), 221–227. doi: Doi10.1038/Ngeo156

439 Rodwell, M. J., & Jung, T.   (2008).   Understanding the local and global impacts
440   of model physics changes: An aerosol example.   *Quarterly Journal of the Royal*
441   *Meteorological Society*, *134*(635), 1479–1497.

442 Simmons, A. J., Wallace, J. M., & Branstator, G. W.   (1983).   *Barotropic wave*
443   *propagation and instability, and atmospheric teleconnection patterns.* (Vol. 40)
444   (No. 6). doi: 10.1175/1520-0469(1983)040⟨1363:BWPAIA⟩2.0.CO;2

445 Song, F. F., Zhou, T. J., & Qian, Y. (2014). Responses of East Asian summer mon-
446   soon to natural and anthropogenic forcings in the 17 latest CMIP5 models.
447   *Geophysical Research Letters*, *41*(2), 596–603. doi: Doi10.1002/2013gl058705

448 Takaya, K., & Nakamura, H.   (2001).   A Formulation of a Phase-Independent Wave-
449   Activity Flux for Stationary and Migratory Quasigeostrophic Eddies on a
450   Zonally Varying Basic Flow.   *Journal of the Atmospheric Sciences*, *58*(6),
451   608–627. doi: 10.1175/1520-0469(2001)058⟨0608:Afoapi⟩2.0.Co;2

452 Tosca, M. G., Randerson, J. T., & Zender, C. S.   (2013).   Global impact of

smoke aerosols from landscape fires on climate and the Hadley circulation. *Atmospheric Chemistry and Physics*, *13*(10), 5227–5241. doi: 10.5194/acp-13-5227-2013

Wallace, J. M., & Gutzler, D. S. (1981). Teleconnections in the geopotential height field during the northern hemisphere winter. *Monthly Weather Review*, *109*(4), 784–812.

Wang, B., & Xie, X. (1996). Low-Frequency Equatorial Waves in Vertically Sheared Zonal Flow. Part I: Stable Waves. *Journal of the Atmospheric Sciences*, *53*(3), 449–467. doi: 10.1175/1520-0469(1996)053⟨0449:Lfewiv⟩2.0.Co;2

Wang, N., & Zhang, Y. (2015). Evolution of eurasian teleconnection pattern and its relationship to climate anomalies in china. *Climate Dynamics*, *44*(3-4), 1017–1028.

Yasunari, T. J., Koster, R. D., Lau, W. K. M., & Kim, K. M. (2015). Impact of snow darkening via dust, black carbon, and organic carbon on boreal spring climate in the Earth system. *Journal of Geophysical Research-Atmospheres*, *120*(11), 5485–5503.

Zhang, H., Wang, Z. L., Wang, Z. Z., Liu, Q. X., Gong, S. L., Zhang, X. Y., . . . Li, L. (2012). Simulation of direct radiative forcing of aerosols and their effects on East Asian climate using an interactive AGCM-aerosol coupled system. *Climate Dynamics*, *38*(7-8), 1675–1693. doi: DOI10.1007/s00382-011-1131-0

Zhu, Z., & Li, T. (2016). A New Paradigm for Continental U.S. Summer Rainfall Variability: Asia–North America Teleconnection. *Journal of the Atmospheric Sciences*, *29*(20), 7313–7327. doi: 10.1175/jcli-d-16-0137.1
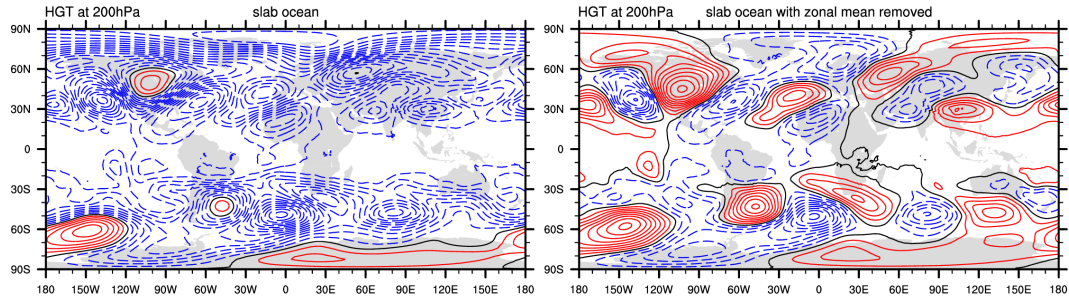
476 # Appendix

Figure A1. the changes in geopotential height at 200hPa induced by wildfire aerosols in February from the simulation with the slab ocean model (contour internal of 5 gpm, analyzed the results of the last 40 years with 20 years spin-up ahead). Left: Fire minus noFire; Right: Fire minus noFire with the zonal mean removed.